Highly Robust Silver Nanowire Network for Transparent Electrode

Tze-Bin Song,[†,‡,#] You Seung Rim,[†,‡,#] Fengmin Liu,[†,‡,§], Brion Bob,[†,‡], Shenglin Ye,[†,‡] Yao-Tsung Hsieh,[†,‡] and Yang Yang[*,†,‡]

[†]Department of Materials Science and Engineering, University of California, Los Angeles, Los Angeles, California 90095, United States, [‡]California NanoSystems Institute, University of California Los Angeles, Los Angeles, CA 90095, United States, and, [§]College of Electronic Science and Engineering, Jilin Univsersity, 2699 Qianjin Street, Changchun 130012, PR China

ABSTRACT

Solution-processed silver nanowire networks are one of the promising candidates to replace a traditional indium tin oxide as the next generation transparent and flexible electrodes due to their ease of processing, moderate flexibility, high transparency and low sheet resistance. To date however, high stability of the nanowire networks remains a major challenge because the long-term usages of these electrodes are limited by their poor thermal and chemical stabilities. Existing methods for addressing this challenge mainly focus on protecting the nanowire network with additional layers that require vacuum processes, which can lead to an increment in manufacturing cost. Here, we report a straightforward strategy of a sol-gel processing as a fast and robust way to improve the stabilities of silver nanowires. Comparing with reported nanoparticles embedded in nanowire networks, better thermal and chemical stabilities are achieved via sol-gel coating of TiO_2 over the silver nanowire networks. The conformal surface coverage suppressed the surface diffusion of silver atoms and prevented the chemical corrosion from the environment. These results highlight the important role of the functional layer to providing better thermal and chemical stabilities along with improved electrical properties and mechanical robustness. The silver nanowires/TiO_2 composite electrodes were applied as the source and drain electrodes for In_2O_3 thin-film transistors (TFTs) and the devices exhibited improved electrical performance annealed at 300°C without the degradation of the electrodes. These key findings not only demonstrated a general and effective method to improve the thermal and chemical stabilities of metal nanowire networks but also provided a basic guideline towards rational design of highly efficient and robust composite electrodes.

KEYWORDS

Transparent electrode, silver nanowire, sol-gel process, stability, thin-film transistor

INTRODUCTION

Transparent conducting electrode is an essential component for most optoelectronic devices and tin-doped indium oxide (ITO) and Al-doped zinc oxide (AZO) are commonly chosen for this layer due to their low resistivity and high transparency in the visible ranges.[1] The manufacture cost of these materials remains high, however, mainly due to the use of vacuum techniques. Therefore, great efforts have been put into solution-processed conductive metal oxides due to its potentially low-cost processing,[2] but high temperature annealing (> 350°C) is required to achieve a conductivity compared with the vacuum process.[3-5] Recently, solution processing of nanowire networks have been developed as a substitute technology for transparent electrodes, such as carbon nanotube (CNT),[6,7] silver nanowire (AgNW)[8,9] and copper nanowire (CuNW).[10,11] High transparency and low sheet resistance films can be obtained through low-temperature solution process (<200°C). In particular, AgNW networks have been attracted attentions as one of promising candidates due to its favorable transmittance, conductance, and flexibility, as compared with the traditional ITO film.[12,13] Poor thermal and chemical stabilities of these metallic nanowires were observed, however, restricting the capability of post-processing and potential applications. The instabilities of the metallic nanowire network are mainly caused by the chemical reaction (including oxidation, sulfurization) and surface diffusion of metal atoms resulting in contact ripening or Rayleigh effect.[14-16] In particular, the ripening at the contacts of the nanowire network causes a discontinuous network, which results in a decreased lifetime and limits post-processing. Some approaches on improving the thermal and chemical stabilities of the nanowire network were proposed using functional protection layers deposited by vacuum techniques such as atomic layer deposition and sputtering[17-19], which although effective led to increased manufacturing cost. Nanoparticles coatings were also reported, although the effectiveness may be limited by the incomplete coverage of the nanoparticles.[20-22] Polymer coatings, such as poly(3,4-ethylenedioxythiophene):poly(styrenesulfonate) (PEDOT:PSS), were reported facing acid

degradation and limited thermal stability to 210°C for 20 min.[23] Reduced graphene oxide and graphene provided moisture protection on AgNW were reported, however, the complicated preparation processes are required and thermal stability in air is still under investigation.[24,25] Therefore, a fast and robust process to improve the thermal and chemical stabilities of the nanowire networks while providing better or equivalent electrical, optical and mechanical properties is needed.

Here, we demonstrated a sol-gel method using titanium dioxide (TiO_2) as a highly efficient protecting layer over the AgNW networks. The sol-gel TiO_2 film has found widespread application in areas such as antireflection coating,[26] wear resistant,[27] and chemical resistant coating.[28] The sol-gel solution process is inexpensive and easily adaptable for industrial mass production. The process can be done in atmospheric conditions and the coating properties can be precisely controlled by tuning the temperature, chemical contents, and molar ratios of the precursors. Moreover, a variety of methods are available for depositing these coatings, such as spin-coating, dipping coating, spray coating, and blade coating. We found that by applying sol-gel TiO_2 onto the AgNW network, the composite electrode showed improved electrical and optical properties, superior performance in thermal stability tests, bending test, chemical corrosion test and exhibited better adhesion with the substrates. During the thermal stability test and chemical stability test, nanowire networks were covered by using a nanoparticle functional layer and bare nanowire networks are examined along with those functionalized by the sol-gel TiO_2 process. The mechanisms of the stability improvements were discussed in the manuscript. To confirm the feasibility of our process, we employed AgNW-sol-gel TiO_2 as the source and drain (S/D) electrodes for solution-processed indium oxide (In_2O_3) thin-film transistors (TFTs) with a bottom-gate structure through the post-annealing process (300°C). Surprisingly, we found that the electrical performance of In_2O_3 TFTs was improved without electrical degradation of S/D electrodes.

RESULTS AND DISCUSSION

Diluted AgNW dispersion was spun onto the target substrate and the result is shown in the scanning electron microscopy (SEM) image in Figure 1a. The titanium isopropoxide ($Ti\{OCH(CH_3)_2\}_4$, TTIP) was diluted with ethanol and a small amount of ethanolamine, and then spun onto the AgNW network. The ethanolamine was added to stabilize the sol preventing it from forming crystalline precipitations. The AgNW-sol-gel TiO_2 composite film was shown with tilted angle SEM in Figure 1b. The details of the experiment were described in the experimental section. The sol-gel TiO_2 layer exhibited a conformal coverage over the entire AgNW network with 100~ 150 nm thickness and showed an amorphous phase due to the room temperature process (X-ray diffraction (XRD) spectra are shown in Figure S1).[29] A thinner layer of sol-gel TiO_2 would not provide a full coverage due to the roughness of the AgNW network. The transmittance and sheet resistance of AgNW-sol-gel TiO_2 film are 85.6% at a wavelength of 550 nm and 13.2 ohm/sq, which are superior to the previous report with a 84% transmittance and a 19 ohm/sq sheet resistance using similar aspect ratio AgNWs (averaged diameter of 90 nm and averaged length 30 μm), as shown in Figure. 1c and d.[16,30,31] Although the transmittance was slightly affected by the sol-gel TiO_2 layer, which has a high transmittance of 99.3% at the wavelength of 550 nm with glass as the reference and an absorption edge showed at around 340 nm (Figure S2), which corresponding to the amorphous TiO_2.[32] It is found that the sheet resistance was significantly reduced after the sol-gel TiO_2 layer deposition even without any heat treatment (Figure 1e). Different with other processes, including thermal annealing, plasmonic welding and current ripening,[16,33-35] the reduction of the sheet resistance in AgNW-sol-gel TiO_2 could be originated from the shrinking force from the gelation process during the evaporation of the solvent and the transformation between TTIP and TiO_2 network during the drying process, and the increasing conductive pathways from sol-gel TiO_2 coating between adjacent AgNWs.[36]

Thermal stability test was done in air under different temperatures with one hour treatment time, as shown in Figure 2. Bare AgNW networks, AgNW networks incorporated with metal oxide nanoparticles (NPs) as the functional protecting material were fabricated and tested in comparison with the sol-gel TiO_2 process.[21,22,37] The sheet resistance of the as fabricated AgNW networks was fixed around 20 ohm/sq while extra coatings with nanoparticles and sol-gel TiO_2 would reduce the sheet resistance to around 11 ohm/sq as shown in Figure 1e.[38] No significant changes in the electrical properties was observed for any one of the three cases during the thermal stability test at 200°C as shown in Figure. 2a. However, when tested at 250°C, the sheet resistance of the bare AgNW film increased rapidly up to values beyond our measurement capacity of 120 Mohm/sq. When the bare AgNW film was treated at 300°C, the conductive pathways within the network was disconnected within 5 min as shown in Figure 2b. Some of the nanowires within the bare AgNW network became small droplets due to contact ripening and Rayleigh instability.[39] Meanwhile, the AgNW-sol-gel TiO_2 composite film remained intact after 10 min at 300°C treatment (Figure 2c). For the AgNW-ITO NPs composite, the ITO NPs provided partial protection to the AgNW network as well as acting as the conductive matrix to the film. The sheet resistance of AgNW-ITO NPs composite increased slower than the bare AgNW network, and saturated to around 10^4 ohm/sq due to the conductive matrix of ITO NPs under 300°C treatment.[40] When the temperature was increased to 350°C, the sheet resistance of the AgNW-sol-gel TiO_2 composite rose gradually to over 120 Mohm/sq in around one hour. Results from higher temperatures (375°C and 400°C) were shown in Figure S3 and it was clearly shown that the AgNW-sol-gel TiO_2 composite maintained its conductive path and sheet resistance value for more than 5 min under 400°C. These results demonstrated that the thermal stability of the AgNW network was significantly improved with the incorporation of sol-gel TiO_2. Previously, it has been reported that by adopting a core-shell AgNW/TiO_2 structure, the single AgNW can be stable up to 750°C in 10 min under ultra high vacuum.[18] In a nanowire network, however, low surface energy grooves

are formed at the contacts between wires and these could facilitate the movement of Ag atoms to the contact through surface and bulk diffusion, causing contact ripening and Rayleigh effect to happen at a lower temperature or shorter treatment time.[16,41] Conformal coating using sol-gel TiO_2 layer over the AgNW network can effectively suppress the surface diffusion and enhance the thermal stability of the network compared with bare AgNW and NP coated composite AgNW networks.

Chemical stability of the AgNW-sol-gel TiO_2 composite electrode was examined through corrosion test comparing these AgNW composite films and bare AgNW network. Although Ag is stable in most chemical environments; it can be easily reacted with sulfur to form Ag_2S, which is black in color.[14] In this case, sulfur was provided dissolved in the solvent dimethylformamide (DMF) and applied to AgNW network with and without functional protecting layers. The AgNW films were soaked into 60 ml of DMF solvent containing 0.008 g of sulfur powders for 30 min. Higher chemical stability was observed for the AgNW-sol-gel TiO_2 composite electrode compared with the bare AgNW network and NPs coated AgNW network, as shown in Figure 3. As shown in Figure 3a, the sheet resistance of the bare AgNW network increased more than six orders of magnitude of its initial resistance value after the 30 min treatment. The sheet resistance increased around three orders of magnitude for the AgNW-NPs composite film and the sheet resistance change in both cases could be attributed to the reaction of Ag with sulfur ion decreasing the amount of the AgNWs present for creating conductive pathways within the AgNW network. The AgNW-sol-gel TiO_2 composite film was slightly affected and the resistance rose to twice its original value. For the bare AgNW case, although the AgNWs kept their original shapes but Energy Dispersive X-ray Spectroscopy (EDS) showed the atomic ratio of silver and sulfur closing to 2:1. This is a clear indication that most of the AgNWs were corroded by the sulfur ions. Meanwhile, the sol-gel TiO_2 covered AgNW network remained intact as observed by SEM and sulfur was not detected by EDS analysis, as shown in Figure 3b and c. (EDS results are shown in the Figure

S4) The three types of AgNW networks investigated behaved differently when placed in a chemical environment containing sulfur and a schematic diagram was shown in Figure 3d. The exposed surface area of the AgNWs determines the reaction rate between silver atoms and sulfur ions, making bare AgNWs most prone to chemical corrosion. NPs in the AgNW-NPs composite electrode could provide partial protection for the AgNWs, however sulfur ions could still penetrate the nanoporous structure and react with the Ag atoms, although at a slower rate compared to the bare AgNW case. The sol-gel layer offered the best corrosion resistance due to its full coverage of the AgNW network and choosing TiO_2 as opposed to other metal oxides such as zinc oxide can provide the additional benefit of being resistant to most base and acid solutions, thereby providing a more chemically stable protection.

Mechanical properties including the adhesion to substrates and flexibility are probed to test this method's compatibility with electronic device fabrication and roll-to-roll processing. The adhesion property was tested by peeling with scotch tape and the resistance of the AgNW films were recorded before and after the taping process (Figure 4a and b). The samples shown on the top of Figure 4a were bare AgNW network film, with a sheet resistance of 4.6 ohm/sq and transmittance of 52.1% at the wavelength of 550 nm. The AgNW-sol-gel TiO_2 composite had a sheet resistance and transmittance of 3.6 ohm/sq and 49.3% repectively. After peel-off test using the scotch tape, the sheet resistance of AgNW-sol-gel TiO_2 did not change. The sheet resistance of the bare AgNW network, however, increased to a value that is beyond our measurement capacity (120 Mohm/sq) due to the weak adhesion between the glass substrate and the AgNW network as shown in Figure 4b. Therefore, the sol-gel TiO_2 performed as a mold to hold the AgNWs to the substrates. Furthermore, the flexibility of the AgNW-sol-gel TiO_2 composite was evaluated through a bending test as shown in the Figure 4c. To compare the AgNW-sol-gel TiO_2 composite film with the standard sputtered ITO electrode, both films were prepared on polyethylene terephthalate (PET) substrates. Five hundred bending cycles with a bending radius of 0.5 cm was applied on both films and the sheet resistance changes

were recorded. Though, the interface between sol-gel TiO_2 and PET substrate is not favorable and the cracks before bending test were observed under the SEM as in Figure S5. The sheet resistance of the AgNW-sol-gel TiO_2 composite film was still maintained after 500 cycles due to the conductive path of AgNW networks. On the other hand, the sheet resistance of the sputtered ITO rapidly increased for even below 100 cycles due to crack formation reducing the conductive path within the ITO film.[42]

The AgNW-sol-gel TiO_2 composite was incorporated into TFT devices as the S/D electrodes to explore its feasibility as a practical electrode. Solution-processed In_2O_3 channel material was formed onto the p+ doped Si wafer with a thermally grown SiO_2 (100 nm), and S/D electrodes were deposited by spray-coating diluted AgNWs and TTIP precursor solutions through shadow masks on top of the In_2O_3 layer. A schematic structure of the device is shown in Figure 5a. A photo of the TFTs was shown in Figure 5b with the inset showing an optical image of one of the device and the channel length and width were measured to be 90 μm and 820 μm, respectively. Transfer curves of In_2O_3 TFTs with before and after thermal treatment were plotted in Figure 5c, and d. As-deposited AgNW-sol-gel TiO_2 electrodes-based In_2O_3 TFTs showed a poor electrical contact and a poor electrical performance, and had the saturation mobility (μ_{sat}) and sub-threshold voltage swing (S.S) of 0.24 $cm^2 \cdot V^{-1} \cdot s^{-1}$ and 1.72 $V \cdot dec^{-1}$, respectively. However, the electrical performance of 300°C annealed In_2O_3 TFTs with AgNW-sol-gel TiO_2 electrodes was significantly improved and the transfer curve showed a better switching behavior, as shown in Figure 5d and S6, with μ_{sat} and S.S of devices showed 1.91 $cm^2 \cdot V^{-1} \cdot s^{-1}$ and 0.80 $V \cdot dec^{-1}$, respectively. 80°C annealed TiO_2 films could contain large amount of hydroxide groups due to incomplete dehydroxylation of precursors.[43] Thus, TiO_2 layer could not contribute to the improved electrical contact to In_2O_3 channel layer (as shown in Figure S1). After 300°C annealing for 10 min in air, TiO_2 precursor could be fully transferred to TiO_2 layer. Typically, TiO_2 was well known as an n-type semiconductor, which could contribute to the carrier transport between AgNWs and

In_2O_3 contact. Furthermore, we speculated that the contact between annealed AgNWs and In_2O_3 was directly improved. Thus, AgNW-sol-gel TiO_2 electrodes showed a better compatibility to TFT application compared with bare AgNW film by improving the thermal stability and electrode lifetime of the devices. Further modifications of the sol-gel TiO_2 layer to improve the device contacts are anticipated to achieve better device performance.[44,45]

CONCLUSIONS AND PROSPECTS

Solution-processed AgNW-sol-gel TiO_2 composite electrode was demonstrated to reduce the sheet resistance of the AgNW network while improving the thermal stability under various temperatures and treatment times over bare AgNW electrodes by suppressing the surface diffusion of silver atoms during the thermal treatment. Sol-gel TiO_2 were also shown to provide excellent chemical corrosion resistance for the AgNW network preventing the sulfurization of silver atoms. Both the thermal stability and chemical stability enhancement highlighted the superior performance of a full coverage layer, compared to bare AgNW networks and AgNW-NPs composite electrode with the NPs forming a nanoporous protection layer. Better thermal and chemical stabilities opened up new possibilities for post-fabrications with high temperatures or harsh chemical conditions. This was demonstrated by applying AgNW-sol-gel TiO_2 composite electrode as the electrode of TFT devices, in which post fabrication annealing successfully improved the observed device performance. Moreover, the sol-gel TiO_2 layer could greatly improved AgNW's adhesion to the substrate and the composite electrodes showed excellent flexibility, making it a promising candidate for flexible electronics.

EXPERIMENTAL METHODS

AgNW composite film preparation. AgNWs were obtained from Blue Nano Inc with an averaged diameter of around 90 nm and an averaged length of around 30 μm. Titanium

isopropoxide ($Ti\{OCH(CH_3)_2\}_4$, TTIP) and ethanolamine were purchased from Sigma Aldrich Inc. Diluted AgNW (2.5 mg/mL) dispersed in ethanol was spun onto the pre-cleaned rigid glass substrates as well as polyethylene terephthalate (PET) flexible substrates (3M Transparency Film, 3M). Diluted AgNW dispersion was spun onto the targeting substrate with a 2000 rpm spin speed. Different AgNW densities are prepared by multiple spin coating cycles. Diluted TTIP solution with ethanol and ethanolamine (volume ratio 1:10:0.1, no aging is required.) was spun onto the AgNW network with 2000 rpm for 40 seconds. The films were baked at 80°C for 5 min to remove the residual solvent. The ITO NPs dispersion was purchased from Sigma Aldrich Inc. and diluted with isopropyl alcohol (IPA). A detail preparation of AgNW-ITO NPs composite film is described in previous reports.[38]

Device fabrication. The devices were fabricated on p+-type silicon wafer with 100 nm SiO_2 layer as the dielectric layer. 0.1 M In_2O_3 solution was synthesized by dissolving indium nitrate hydrate ($In(NO_3)_3 \cdot xH_2O$, Aldrich, 99.999%) in water (H_2O, Aldrich).[46] The In_2O_3 precursor solution was spin-coated on substrates at 3000 rpm for 30 s. The samples were then soft-baked at 100 °C for 5 min to eliminate water and then annealed at 300°C for 3 h. The annealed samples were patterned using the photolithography process. Diluted AgNW dispersion was deposited by spray-coating using a mask with 150 μm defined channel length onto the In_2O_3 layer at 80°C. The diluted TTIP solution was sprayed onto the AgNW network in room temperature and then baked at 80 and 300°C for 10 min, respectively.

Optical, electrical, and structural characterization. XRD data were collected on Panalytical X'Pert Pro X-ray Powder Diffractometer with Cu Kα radiation (λ=1.54056 Å). Optical specular transmittance of the films was measured using a Hitachi Ultraviolet–Visible Spectrophotometer (U-4100) without an integrating sphere. The measured transmittance values exclude scattered light and Fresnel reflection. A glass substrate was used as a reference in the transmittance measurement. The surface resistance (<100 ohm/sq) was measured using a four-point probe method with a surface resistivity meter (Guardian Guardian Manufacturing,

Model: SRM-232-100, range: 0~100 ohm/sq). Two-point probe method was used to estimate the surface resistance of the film with surface resistance >100 ohm/sq. TFTs were measured by a semiconductor parameter analyzer (Agilent 4155C, Agilent Technologies) connected to a probe station. SEM images were taken on a JEOL JSM-6700F electron microscope.

ASSOCIATED CONTENT

Supporting Information. XRD and transmission of the sol-gel TiO_2 films, sheet resistance changes of AgNW-sol-gel TiO_2 electrode versus annealing time under different temperature, EDS characterization of AgNW after chemical environment reaction, SEM images of sol-gel TiO_2 layer and AgNW-sol-gel TiO_2 composite on PET substrates, and I_D-V_D curve of TFT of In_2O_3 after thermal annealing are in Figure S1 to S6. This material is available free of charge *via* the Internet at http://pubs.acs.org.

AUTHOR INFORMATION

Corresponding Authors

yangy@ucla.edu (Y. Y.)

Author Contributions

[#]T.-B. S and Y. S. R. contributed equally to this work.

Conflict of Interests

The authors declare no competing financial interests.

ACKNOWLEDGEMENTS

The authors would like to express their gratitude for the generous financial support from the National Science Foundation (grant no. ECCS-1202231, Program Director Dr. Paul Werbos) and UCLA Internal Funds.

REFERENCES

1. Gordon, R. G. Criteria for Choosing Transparent Conductors. *MRS Bulletin* **2000**, *25*, 52-57.

2. Thomas, S. R.; Pattanasattayavong, P.; Anthopoulos, T. D. Solution-Processable Metal Oxide Semiconductors for Thin-Film Transistor Applications. *Chem. Soc. Rev.* **2013**, *42*, 6910-6923.

3. Nadarajah, A.; Carnes, M. E.; Kast, M. G.; Johnson, D. W.; Boettcher, S. W. Aqueous Solution Processing of F-Doped SnO_2 Transparent Conducting Oxide Films Using a Reactive Tin Hydroxide Nitrate Nanoscale Cluster. *Chem. Mater.* **2013**, *25*, 4080-4087.

4. Chen, Z.; Li, W.; Li, R.; Zhang, Y.; Xu, G.; Cheng, H. Fabrication of Highly Transparent and Conductive Indium Tin Oxide Thin Films with a High Figure of Merit *via* Solution Processing. *Langmuir* **2013**, 29, 13836-13842.

5. Kim, N.-R.; Lee, J.-H.; Lee, Y.-Y.; Nam, D.-H.; Yeon, H.-W.; Lee, S.-Y.; Yang, T.-Y.; Lee, Y.-J.; Chu, A.; Nam, K. T.; Joo, Y.-C. Enhanced Conductivity of Solution-Processed Indium Tin Oxide Nanoparticle Films by Oxygen Partial Pressure Controlled Annealing. *J. Mater. Chem. C* **2013**, 1, 5953-5959.

6. De Volder, M. F. L.; Tawfick, S. H.; Baughman, R. H.; Hart, A. J. Carbon Nanotubes: Present and Future Commercial Applications. *Science* **2013**, 339, 535-539.

7. Hu, L.; Hecht, D. S.; Gruner, G. Carbon Nanotube Thin Films: Fabrication, Properties, and Applications. *Chem. Rev.* **2010**, 110, 5790-5844.

8. Lee, J.-Y.; Connor, S. T.; Cui, Y.; Peumans, P. Solution-Processed Metal Nanowire Mesh Transparent Electrodes. *Nano Lett.* **2008**, 8, 689-692.

9. Song, T.-B.; Li, N. Emerging Transparent Conducting Electrodes for Organic Light Emitting Diodes. *Electronics* **2014**, 3, 190-204.

10. Ye, S.; Rathmell, A. R.; Stewart, I. E.; Ha, Y.-C.; Wilson, A. R.; Chen, Z.; Wiley, B. J. A Rapid Synthesis of High Aspect Ratio Copper Nanowires for High-Performance Transparent Conducting Films. *Chem. Commun.* **2014**, 50, 2562-2564.

11. Rathmell, A. R.; Wiley, B. J. The Synthesis and Coating of Long, Thin Copper Nanowires to Make Flexible, Transparent Conducting Films on Plastic Substrates. *Adv. Mater.* **2011**, 23, 4798-4803.

12. Leem, D.-S.; Edwards, A.; Faist, M.; Nelson, J.; Bradley, D. D. C.; de Mello, J. C. Efficient Organic Solar Cells with Solution-Processed Silver Nanowire Electrodes. *Adv. Mater.* **2011**, 23, 4371-4375.

13. Song, M.; You, D. S.; Lim, K.; Park, S.; Jung, S.; Kim, C. S.; Kim, D.-H.; Kim, D.-G.; Kim, J.-K.; Park, J.; Kang, Y.-C.; Heo, J.; Jin, S.-H.; Park, J. H.; Kang, J.-W. Highly Efficient and Bendable Organic Solar Cells with Solution-Processed Silver Nanowire Electrodes. *Adv. Funct. Mater.* **2013**, 23, 4177-4184.

14. Elechiguerra, J. L.; Larios-Lopez, L.; Liu, C.; Garcia-Gutierrez, D.; Camacho-Bragado, A.; Yacaman, M. J. Corrosion at the Nanoscale: The Case of Silver Nanowires and Nanoparticles. *Chem Mater.* **2005,** 17, 6042-6052.

15. Karim, S.; Toimil-Molares, M. E.; Ensinger, W.; Balogh, A. G.; Cornelius, T. W.; Khan, E. U.; Neumann, R. Influence of Crystallinity on the Rayleigh Instability of Gold Nanowires. *J. Phys. D: Appl. Phys.* **2007,** 40, 3767.

16. Song, T.-B.; Chen, Y.; Chung, C.-H.; Yang, Y.; Bob, B.; Duan, H.-S.; Li, G.; Tu, K.-N.; Huang, Y.; Yang Y. Nanoscale Joule Heating and Electromigration Enhanced Ripening of Silver Nanowire Contacts. *ACS Nano* **2014,** 8, 2804-2811.

17. Hsu, P.-C.; Wu, H.; Carney, T. J.; McDowell, M. T.; Yang, Y.; Garnett, E. C.; Li, M.; Hu, L.; Cui, Y. Passivation Coating on Electrospun Copper Nanofibers for Stable Transparent Electrodes. *ACS Nano* **2012,** 6, 5150-5156.

18. Ramasamy, P.; Seo, D.-M.; Kim, S.-H.; Kim, J. Effects of TiO_2 Shells on Optical and Thermal Properties of Silver Nanowires. *J. Mater. Chem.* **2012**, 22, 11651-11657.

19. Zilberberg, K.; Gasse, F.; Pagui, R.; Polywka, A.; Behrendt, A.; Trost, S.; Heiderhoff, R.; Görrn, P.; Riedl, T. Highly Robust Indium-Free Transparent Conductive Electrodes Based on Composites of Silver Nanowires and Conductive Metal Oxides. *Adv. Funct. Mater.* **2014**, 24, 1671-1678.

20. Ghosh, D. S.; Chen, T. L.; Mkhitaryan, V.; Formica, N.; Pruneri, V. Solution Processed Metallic Nanowire Based Transparent Electrode Capped with a Multifunctional Layer. *Appl. Phys. Lett.* **2013**, 102, 221111.

21. Shen, G.-H.; Hong, F. C.-N. Ultraviolet Photosensors Fabricated with Ag Nanowires Coated with ZnO Nanoparticles. *Thin Solid Films* **2014**, 570, 363-370.

22. Morgenstern, F. S. F.; Kabra, D.; Massip, S.; Brenner, T. J. K.; Lyons, P. E.; Coleman, J. N.; Friend, R. H. Ag-Nanowire Films Coated with ZnO Nanoparticles as a Transparent Electrode for Solar Cells. *Appl. Phys. Lett.* **2011**, 99, 183307.

23. Chen, S.; Song, L.; Tao, Z.; Shao, X.; Huang, Y.; Cui, Q.; Guo, X. Neutral-Ph PEDOT:PSS as Over-Coating Layer for Stable Silver Nanowire Flexible Transparent Conductive Films. *Org. Electon.* **2014**, 15, 3654-3659.

24. Ahn, Y.; Jeong, Y.; Lee, Y. Improved Thermal Oxidation Stability of Solution-Processable Silver Nanowire Transparent Electrode by Reduced Graphene Oxide. *ACS Appl. Mater. Interfaces* **2012**, 4, 6410-6414.

25. Lee, D.; Lee, H.; Ahn, Y.; Jeong, Y.; Lee, D.-Y.; Lee, Y. Highly Stable and Flexible Silver Nanowire-Graphene Hybrid Transparent Conducting Electrodes for Emerging Optoelectronic Devices. *Nanoscale* **2013**, 5, 7750-7755.

26. Langlet, M.; Burgos, M.; Coutier, C.; Jimenez, C.; Morant, C.; Manso, M. Low Temperature Preparation of High Refractive Index and Mechanically Resistant Sol-Gel TiO_2 Films for Multilayer Antireflective Coating Applications. *J. Sol-Gel Sci. Tech.* **2001**, 22, 139-150.

27. Szalkowska, E.; Gluszek, J.; Masalski, J.; Tylus, W. Structure and Protective Properties of TiO_2 Coatings Obtained Using the Sol-Gel Technique. *J. Mater. Sci. Lett.* **2001**, 20, 495-497.

28. Lima Neto, P.; Atik, M.; Avaca, L.; Aegerter, M. Sol-Gel Coatings for Chemical Protection of Stainless Steel. *J. Sol-Gel Sci. Tech.* **1994**, 2, 529-534.

29. La Notte, L.; Salamandra, L.; Zampetti, A.; Brunetti, F.; Brown, T. M.; Di Carlo, A.; Reale, A. Airbrush Spray Coating of Amorphous Titanium Dioxide for Inverted Polymer Solar Cells. *Int. J. Photoenergy* **2012**, 2012, 1-5.

30. Zhu, R.; Chung, C.-H.; Cha, K. C.; Yang, W.; Zheng, Y. B.; Zhou, H.; Song, T.-B.; Chen, C.-C.; Weiss, P. S.; Li, G.; Yang, Y. Fused Silver Nanowires with Metal Oxide Nanoparticles and Organic Polymers for Highly Transparent Conductors. *ACS Nano* **2011**, 5, 9877-9882.

31. Yu, Z.; Li, L.; Zhang, Q.; Hu, W.; Pei, Q. Silver Nanowire-Polymer Composite Electrodes for Efficient Polymer Solar Cells. *Adv. Mater.* **2011**, 23, 4453-44577.

32. Bernardi, M. I. B.; Lee, E. J. H.; Lisboa-Filho, P. N.; Leite, E. R.; Longo, E.; Varela, J. A. TiO_2 Thin Film Growth Using the MOCVD Method. *Mater. Res.* **2001,** 4, 223-226.

33. Garnett, E. C.; Cai, W.; Cha, J. J.; Mahmood, F.; Connor, S. T.; Greyson Christoforo, M.; Cui, Y.; McGehee, M. D.; Brongersma, M. L. Self-Limited Plasmonic Welding of Silver Nanowire Junctions. *Nature Mater.* **2012**, 11, 241-249.

34. Hu, L.; Kim, H. S.; Lee, J.-Y.; Peumans, P.; Cui, Y. Scalable Coating and Properties of Transparent, Flexible, Silver Nanowire Electrodes. *ACS Nano* **2010**, 4, 2955-2963.

35. Ye, S.; Rathmell, A. R.; Chen, Z.; Stewart, I. E.; Wiley, B. J. Metal Nanowire Networks: The Next Generation of Transparent Conductors. *Adv. Mater.* **2014,** 26, 6670-6687.

36. Hench, L. L.; West, J. K. The Sol-Gel Process. *Chem. Rev.* **1990**, 90, 33-72.

37. Kim, A.; Won, Y.; Woo, K.; Jeong, S.; Moon, J. All-Solution-Processed Indium-Free Transparent Composite Electrodes Based on Ag Nanowire and Metal Oxide for Thin-Film Solar Cells. *Adv. Funct. Mater.* **2014**, 24, 2462-2471.

38. Chung, C.-H.; Song, T.-B.; Bob, B.; Zhu, R.; Yang, Y. Solution-Processed Flexible Transparent Conductors Composed of Silver Nanowire Networks Embedded in Indium Tin Oxide Nanoparticle Matrices. *Nano Res.* **2012**, 5, 805-814.

39. Karim, S.; Toimil-Molares, M. E.; Balogh, A. G.; Ensinger, W.; Cornelius, T. W.; Khan, E. U.; Neumann, R. Morphological Evolution of Au Nanowires Controlled by Rayleigh Instability. *Nanotechnology* **2006**, 17, 5954-5959.

40. Chung, C.-H.; Song, T.-B.; Bob, B.; Zhu, R.; Duan, H.-S.; Yang, Y. Silver Nanowire Composite Window Layers for Fully Solution-Deposited Thin-Film Photovoltaic Devices. *Adv. Mater.* **2012**, 24, 5499-5504.

41. Iwama, S.; Hayakawa, K. Sintering of Ultrafine Metal Powders. Ii. Neck Growth Stage of Au, Ag, Al and Cu. *Jap. J. Appl. Phys.* **1981**, 20, 335-340.

42. Peng, C.; Jia, Z.; Neilson, H.; Li, T.; Lou, J. In Situ Electro-Mechanical Experiments and Mechanics Modeling of Fracture in Indium Tin Oxide-Based Multilayer Electrodes. *Adv. Eng. Mater.* **2012**, 15, 250-256.

43. Rim, Y. S.; Jeong, W. H.; Kim, D. L.; Lim, H. S.; Kim, K. M.; Kim, H. J. Simultaneous Modification of Pyrolysis and Densification for Low-Temperature Solution-Processed Flexible Oxide Thin-Film Transistors. *J. Mater. Chem.* **2012,** 22, 12491-12497.

44. Zhu, X.; Kawaharamura, T.; Stieg, A. Z.; Biswas, C.; Li, L.; Ma, Z.; Zurbuchen, M. A.; Pei, Q.; Wang, K. L. Atmospheric and Aqueous Deposition of Polycrystalline Metal

Oxides Using Mist-CVD for Highly Efficient Inverted Polymer Solar Cells. *Nano Lett.* **2015**, 15, 4948-4954.

45. Bob, B.; Song, T.-B.; Chen, C.-C.; Xu, Z.; Yang, Y. Nanoscale Dispersions of Gelled SnO_2: Material Properties and Device Applications. *Chem. Mater.* **2013**, 25, 4725-4730.

46. Rim, Y. S.; Chen, H.; Song, T.-B.; Bae, S.-H.; Yang, Y. Hexaaqua Metal Complexes for Low-Temperature Formation of Fully Metal Oxide Thin-Film Transistors. *Chem. Mater.* **2015,** 27, 5808-5812.

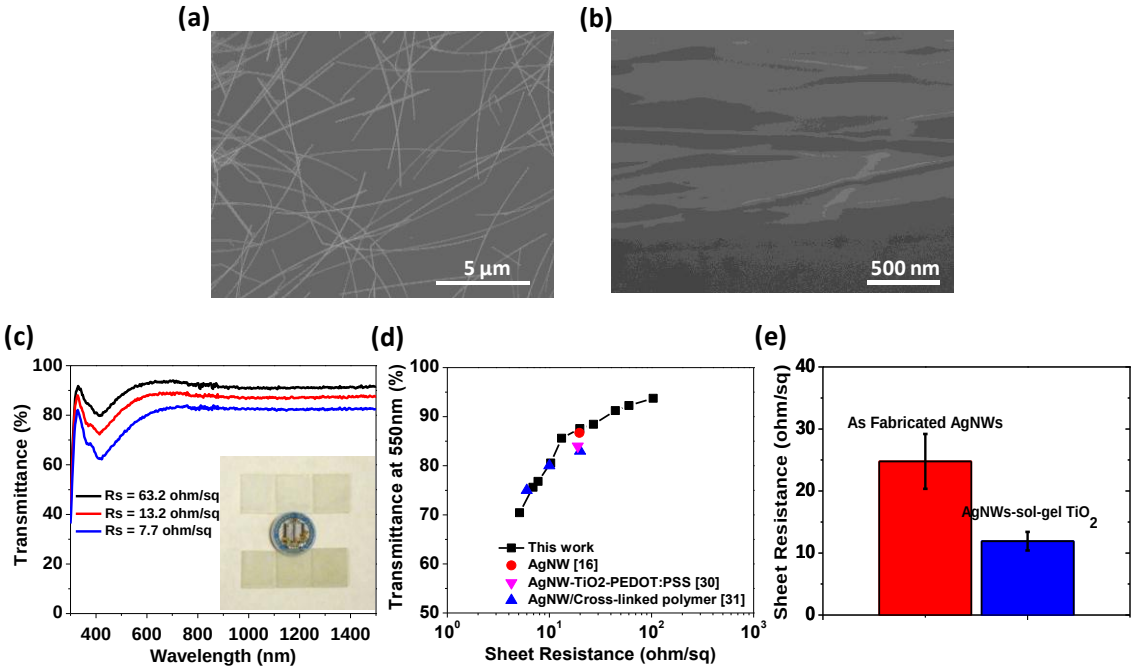

Figure 1. (a) Plain view SEM image of the AgNW network with the average diameter and length of 90 nm and 40 µm. (b) Tilted angle view image of AgNW network covered with sol-gel TiO_2 shows a uniform coverage. (c) The transmittance of the AgNW-sol-gel TiO_2 films over three different sheet resistance values from different AgNW density. The inset shows the optical image of different transmittance films by tuning the AgNW density. (d) Transmittance versus the sheet resistance of AgNW-sol-gel TiO_2 films and literature values of AgNW and AgNW composites. (e) Sheet resistance change before and after sol-gel TiO_2 coating. After sol-gel deposition, averaged sheet resistance of 24 ohm/sq for the as-fabricated AgNW network reduced to averaged sheet resistance of 11 ohm/sq.

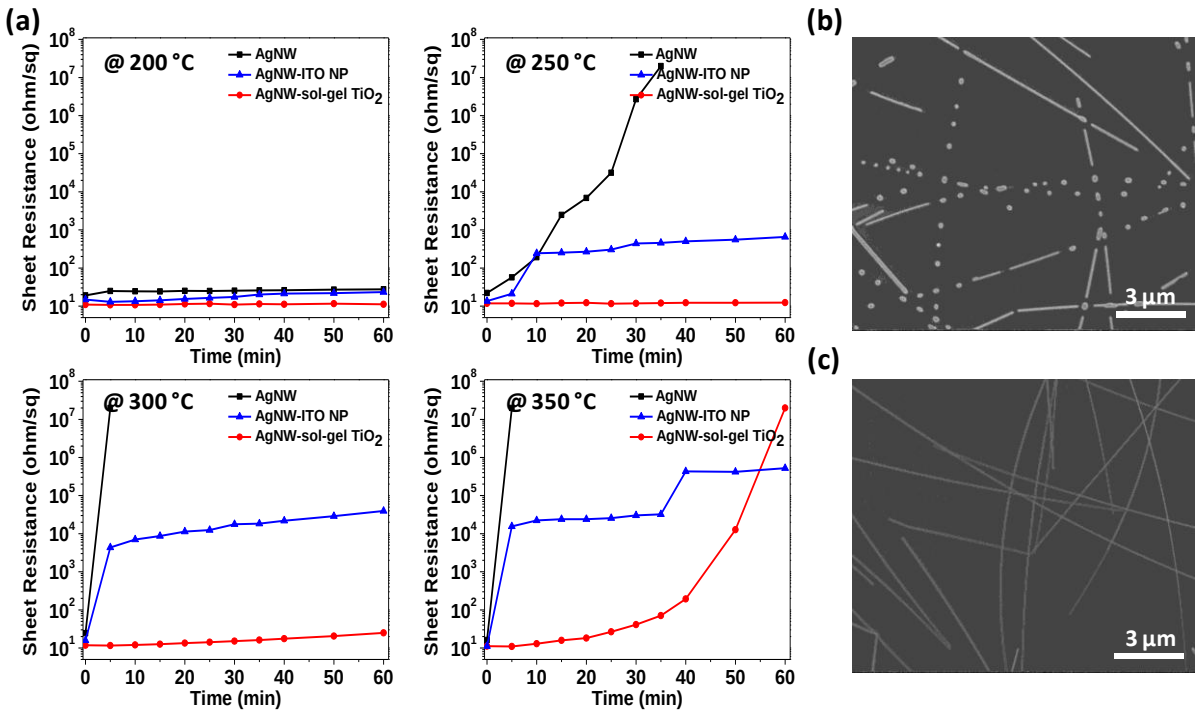

Figure 2. (a) The sheet resistance versus time was recorded under different temperature treatments for bare AgNW networks and two different AgNW composite films, representing unprotected (AgNW), partially protected (AgNW-ITO NPs) and fully protected (AgNW-sol-gel TiO_2) AgNW networks. (b) Plane view SEM images of the bare AgNW network treated at 300°C for 5 min and (c) AgNW-sol-gel TiO_2 film treated at 300°C for 10 min.

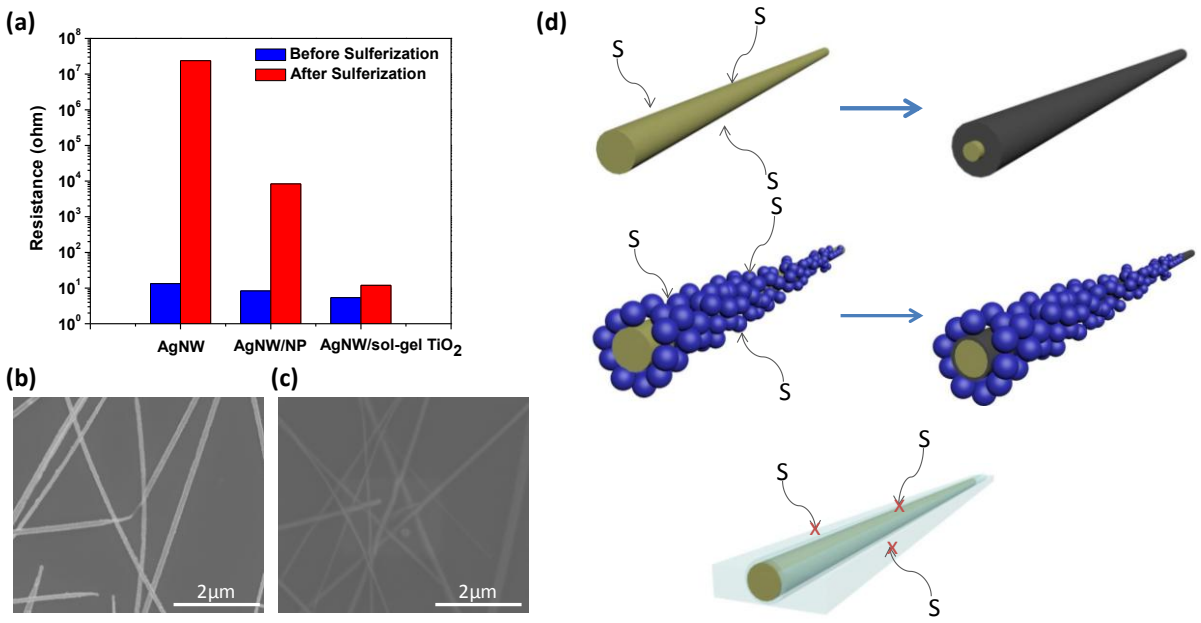

Figure 3. Corrosion test to AgNW and AgNW composite films soaked in the DMF-Sulfur power for 30 min. (a) The sheet resistances changed before and after the sulfurization. (b,c) SEM images of the bare AgNW network and AgNW-sol-gel TiO_2 composite film after sulfurization. (d) The schematic diagrams of the protection mechanism for different cases. The exposure of AgNWs to sulfur ions caused the chemical reaction forming Ag_2S (dark grey color). The reaction rate is proportional to the exposured area. The NPs coating is porous structure and sulfur ions can react with AgNWs. The sol-gel TiO_2 can fully cover around the AgNWs and protect AgNWs from chemical reaction.

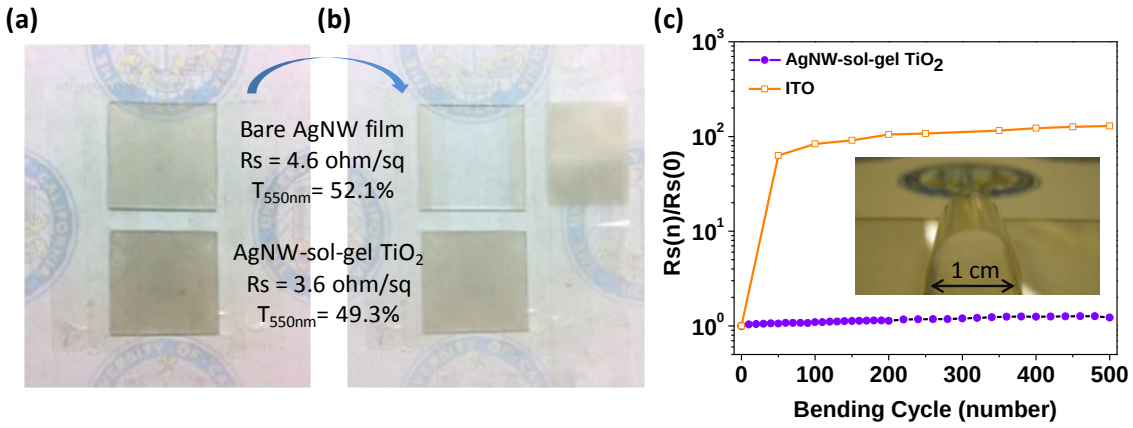

Figure 4. Photos of bare AgNW (top) films and AgNW-sol-gel TiO_2 (bottom) before (a) and after tape test (b). The high densities of AgNW films were used to have a better contrast of the images. The sheet resistance of the bare AgNW films was 4.6 ohm/sq and the AgNW-sol-gel TiO_2 was 3.6 ohm/sq. After adhesion test, the AgNW-sol-gel TiO_2 remained conductive and the bare AgNW was peeled from the substrate. The scotch tape was placed on the right hand side of the samples in (b). (c) Variations in the sheet resistance of AgNW-sol-gel TiO_2 and sputtered ITO film on PET substrates as a function of number of cycles of bending to a 0.5 cm radius curvature. The sheet resistance values were measured after the substrate was relaxed back to planar shape.

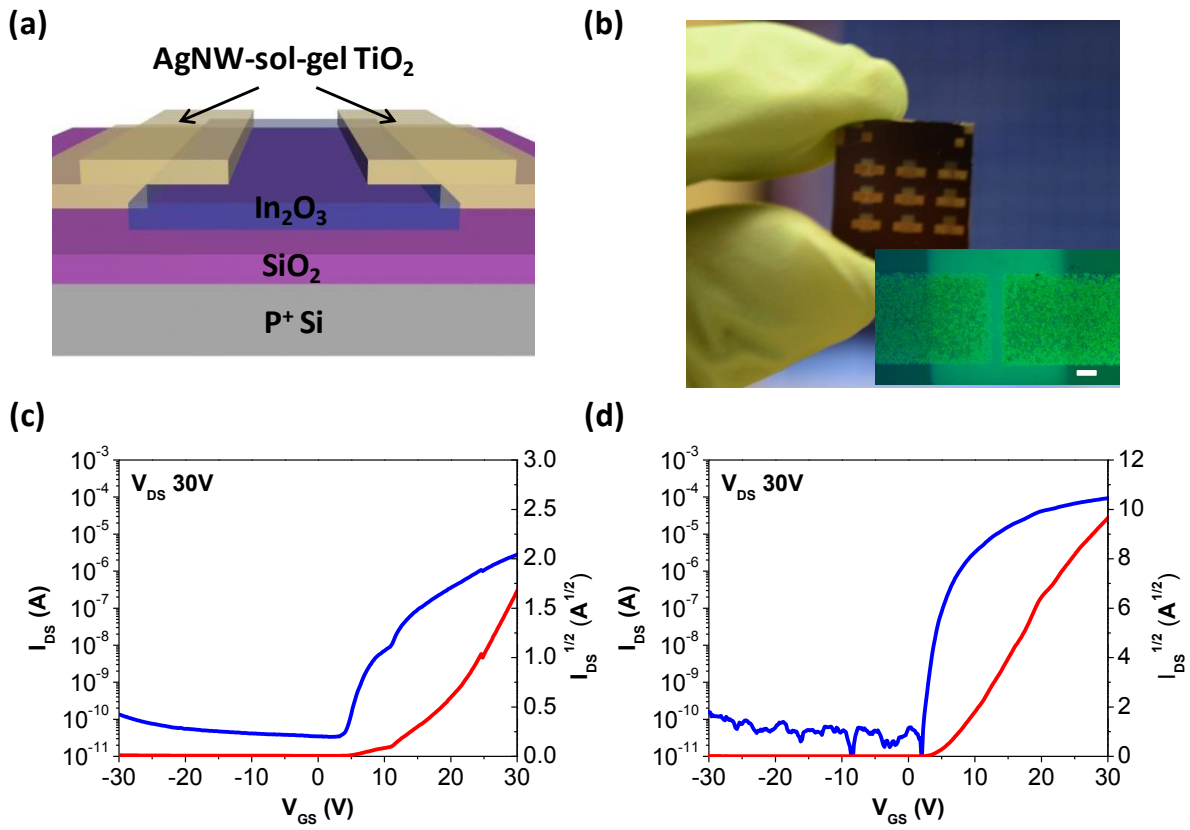

Figure 5. (a) Schematic diagram of the AgNW-sol-gel TiO_2 electrode TFT structure and (b) optical images of the TFT devices. The scale bar is 100 μm. The transfer curves of In_2O_3 TFTs with (c) as-fabricated AgNW-sol-gel TiO_2 electrodes and (d) after baking at 300°C for 10 min under different gate voltage.